2011 American Control Conference
on O'Farrell Street, San Francisco, CA, USA
June 29 - July 01, 2011

Engine Power Smoothing Energy Management Strategy for a Series Hybrid Electric Vehicle

S. Di Cairano, W. Liang, I.V. Kolmanovsky, M.L. Kuang, A.M. Phillips

Abstract— **Hybrid electric vehicles exploit energy production and energy storage systems to achieve improved fuel economy with respect to conventional powertrains. In order to maximize such improvements, advanced control strategies are needed for deciding the amount of energy to be produced and stored. In this paper we propose an approach for energy management of a series hybrid electric vehicle (SHEV). This approach focuses on maximizing the pointwise powertrain efficiency, rather than the overall fuel consumption. For a given power request the steady state engine operating point is chosen to maximize the efficiency. A control algorithm regulates the transitions between different operating points, by using the battery to smoothen the engine transients. Due to the constrained nature of the transient smoothing problem, we implement the control algorithm by model predictive control. Experimental testing on the UDDS cycle shows improved fuel economy with respect to two baseline strategies.**

I. Introduction

Hybrid Electric Vehicles (HEVs) achieve higher fuel economy than conventional vehicles due to the capability of recovering energy during braking, and of using electric batteries to improve the efficiency of the internal combustion engine operation. HEV energy management [1] focuses on deciding how much power should be produced by the internal combustion engine and how much should be stored/released from the auxiliary energy storage systems to achieve the desired power at the wheels, to enforce the operating constraints, and to optimize fuel economy.

In recent years, several strategies for HEV energy management have been proposed, including dynamic programming (DP) [2], stochastic dynamic programming (SDP) [3], equivalent fuel consumption minimization (ECMS) [4], and model predictive control (MPC) [5], [6]. These strategies optimize the fuel economy by solving a problem where the fuel consumption explicitly appears in the cost function. Indeed, this results in minimum fuel consumption if the full information problem can be solved over the whole driving cycle (as in the DP approach). However, information about the future driving cycle is not available during conventional driving. In addition, planning for the whole future driving cycle is computationally demanding. While the use of stochastic models (as in SDP and in stochastic MPC [7]) alleviates some of these problems, the choice of stochastic model and its identification still poses several challenges.

S. Di Cairano is with Powertrain Control R&A, Ford Research and Adv. Engineering, dicairano@ieee.org, sdicaira@ford.com

W. Liang, M.L. Kuang, and A.M. Phillips, are with Sustainable Mobility Technologies, Ford Research and Adv. Engineering, wliang3,mkuang,aphilli8@ford.com

I.V. Kolmanovsky, is with Dept. Aerospace Engineering, University of Michigan, ilya@umich.edu

In this paper we describe a different approach for HEV energy management, and we apply it to a Series Hybrid Electric Vehicle (SHEV). Instead of explicitly optimizing the fuel consumption, we aim at improving the efficiency of the engine operation. Since in the SHEV configuration the engine is mechanically decoupled from the wheels, for a given power request the steady state engine operating point -engine speed and engine torque- can be arbitrarily chosen within a curve. Thus, a curve of optimal operating points as a function of the requested generator power can be computed, and the engine operating point can be controlled to be on that curve in steady state. However, during the transients the engine dynamics move the operating point away from the optimal curve. In this paper we propose to use the battery to "smoothen" the transients so that the engine operating point slides in a narrow band along the optimal efficiency curve.

In order to obtain the engine power smoothing behavior, a Model Predictive Control (MPC) algorithm [8] is implemented. While alternative control designs can also be considered, MPC provides the appealing capabilities of enforcing constraints on the control signals and on the system states, and of defining the priority between the different objectives by a cost function. By multiparametric programming [9] the MPC controller can be synthesized as a feedback law suitable for implementation in engine control units.

In this paper, we discuss the series hybrid vehicle configuration, with particular focus on the power flows, in Section II. In Section III we introduce and motivate the engine power smoothing energy management strategy, and in Section IV we design the feedback controller that implements it. In Section V we discuss the tuning, done in simulation, and we present the experimental results. Conclusions are summarized in Section VI.

II. Series Hybrid Electric Vehicle Architecture

We consider the Series Hybrid Electric Vehicle (SHEV) configuration, shown in Figure 1. In this configuration, the engine powers an electric generator that feeds a DC-bus, which is connected to the battery and to the electric motor. In the SHEV, the electric motor is the unique traction source,

$$P_{\rm wh}(t) = \eta_{\rm wh}(t) P_{\rm mot}(t), \tag{1}$$

where $P_{\rm wh}$ is the power at the wheels, $P_{\rm mot}$ is the electric motor power output, and $\eta_{\rm wh}$ is the (time varying) efficiency in transmitting the mechanical power from the motor to the wheels. Depending on the power flow direction, $\eta_{\rm wh}(t)$ is smaller or greater than 1. The motor power is

$$P_{\rm mot}(t) = \eta_{\rm mot}(t)(P_{\rm gen}(t) + P_{\rm bat}(t)), \tag{2}$$

978-1-4577-0079-8/11/$26.00 ©2011 AACC

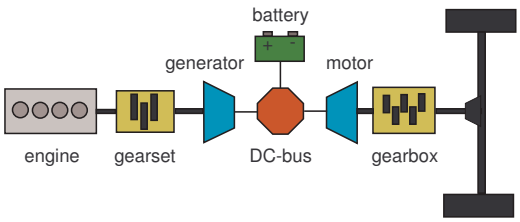

Fig. 1. Schematics of a series hybrid electric powertrain.

where $P_{\rm gen}$ is the generator power, $\eta_{\rm mot}$ is the (varying) motor efficiency, and $P_{\rm bat}$ is the power flow in the bus from the battery. The power coupling occurs in a voltage controlled DC-bus, that has almost perfect efficiency and does not impose mechanical constraints.

The battery power flow changes the charge in the battery ($Q_{\rm bat}$). Since the net power fed by the battery in the bus is $P_{\rm bat} = i_{\rm bus} V_{\rm bus}$, where $i_{\rm bus}$ is the battery current in the bus, and $V_{\rm bus}$ is the (controlled) DC-bus voltage, we have

$$\frac{d}{dt} Q_{\rm bat}(t) = -i_{\rm bat}(t) = -\frac{P_{\rm bat}(t)}{\eta_{\rm bat}(t) V_{\rm bus}(t)}, \tag{3}$$

where $\eta_{\rm bat}$ is the battery efficiency, which accounts for power losses in the circuit and in the battery. The electrical generator is powered by the internal combustion engine

$$P_{\rm gen}(t) = \eta_{\rm gen}(t) P_{\rm eng}(t), \tag{4}$$

where $\eta_{\rm gen}$ is the generator efficiency, and $P_{\rm eng}$ is the engine net power output. The efficiencies $\eta_{\rm gen}$, $\eta_{\rm mot}$, $\eta_{\rm wh}$ can be conveniently represented as functions of the rotational speed and torque of the respective component.

In terms of power flow, for wheel power request there is only one degree of freedom. For instance, if the power released from the battery is selected, then the engine power is assigned by (1), (2), (4). When selecting the engine operating point -engine speed and torque-, an additional degree of freedom is available, since $P_{\rm eng}(t) = \omega_{\rm eng}(t)\tau_{\rm eng}(t)$. Given that there is no mechanical coupling between the different power paths, the selection of the engine operating point can focus only on the engine and generator combined efficiency. For a given engine power,

$$P_{\rm fuel} = \frac{P_{\rm eng}}{\eta_{\rm eng}(\omega_{\rm eng}, \tau_{\rm eng})}, \tag{5}$$

where $P_{\rm fuel}$ is the amount of net power that can be extracted from the fuel burnt in the cylinder, and $\eta_{\rm eng}(\omega_{\rm eng}, \tau_{\rm eng})$ is the engine efficiency map, as a function of the engine speed and engine torque. The fuel consumption is modelled by the relation $P_{\rm fuel} = H_f w_f$, where H_f is the lower fuel lower heating value, and w_f is the fuel mass flow.

For a (desired) engine power output, from (5) the fuel consumption is minimized by selecting the operating point that provides the maximum efficiency. For the SHEV, this is applied to the engine-generator cascade. Consider a gear with ratio κ between the engine and the generator,

$$P_{\rm fuel} = \frac{P_{\rm gen}}{\eta_{\rm gen}\left(\kappa^{-1}\omega_{\rm eng}, \kappa\tau_{\rm eng}\right)\eta(\omega_{\rm eng}, \tau_{\rm eng})}, \tag{6}$$

and define the system efficiency as

$$\eta_{\rm sys}(\omega_{\rm eng}, \tau_{\rm eng}) = \eta_{\rm gen}\left(\kappa^{-1}\omega_{\rm eng}, \kappa\tau_{\rm eng}\right)\eta(\omega_{\rm eng}, \tau_{\rm eng})\,.$$

Given a desired generator power $P_{\rm gen}$, the engine operating point that minimizes the fuel consumption at steady state is obtained by maximizing the efficiency

$$\zeta^*_{\rm sys}(P_{\rm gen}) = \arg\max_{\omega_{\rm eng}, \tau_{\rm eng}} \eta_{\rm sys}(\omega_{\rm eng}, \tau_{\rm eng}) \tag{7a}$$

$$\text{s.t.} \quad \eta_{\rm gen}\left(\frac{\omega_{\rm eng}}{\kappa}, \kappa\tau_{\rm eng}\right)\omega_{\rm eng}\tau_{\rm eng} = P_{\rm gen}. \tag{7b}$$

The curve $\zeta^*_{\rm sys} : \mathbb{R}_+ \to \mathbb{R}^2_+$ assigns the engine operating point with maximum stationary efficiency to the generator power. The efficiency along $\zeta^*_{\rm sys}$ is described by

$$\eta^*_{\rm sys}(P_{\rm gen}) = \max_{\omega_{\rm eng}, \tau_{\rm eng}} \eta_{\rm sys}(\omega_{\rm eng}, \tau_{\rm eng}) \tag{8a}$$

$$\text{s.t.} \quad \eta_{\rm gen}\left(\frac{\omega_{\rm eng}}{\kappa}, \kappa\tau_{\rm eng}\right)\omega_{\rm eng}\tau_{\rm eng} = P_{\rm gen} \tag{8b}$$

In case of a gearbox between engine and generator, (7) and (8) can be modified to select also the optimal gear. Thus, the stationary operating point for a desired generator power is chosen by (7), but the effects of the transients still have to be accounted for. Differently from conventional vehicles, in hybrid powertrains the engine is not the only available energy source, and the redundancy can be used to optimize the transients, as described next.

III. Power Smoothing Control Energy Management

In the considered HEV control architecture, the energy management strategy specifies a target operating point for the energy sources, and several control algorithms drive the subsystems to such operating points, for instance by modulating the battery current and the engine torque. As discussed in Section II, in a SHEV, given two desired generator power levels P_1 and P_2, two optimal engine operating points can be computed. However, if the generator power output varies from P_1 to P_2, the efficiency depends on how the transient is executed.

While the dynamics in the electrical circuit are fast, hence the battery respond quickly to power variations, large "power jumps" in the engine-generator system, may take a considerable time to complete (in the order of seconds). During the transient, the engine is not guaranteed to operate along the maximum efficiency curve $\zeta^*_{\rm sys}$. In Figure 2(a) we show the simulation of the engine operating point dynamics obtained by executing two step power changes (from 2kW to 35kW, and then to 15kW). The simulation is executed on a high-fidelity model that co-simulate the whole powertrain and vehicle dynamics together with the control software including the controller that aims at regulating the engine operating point on $\zeta^*_{\rm sys}$. During the transient the engine runs considerably distant from the optimal efficiency curve $\zeta^*_{\rm sys}$,

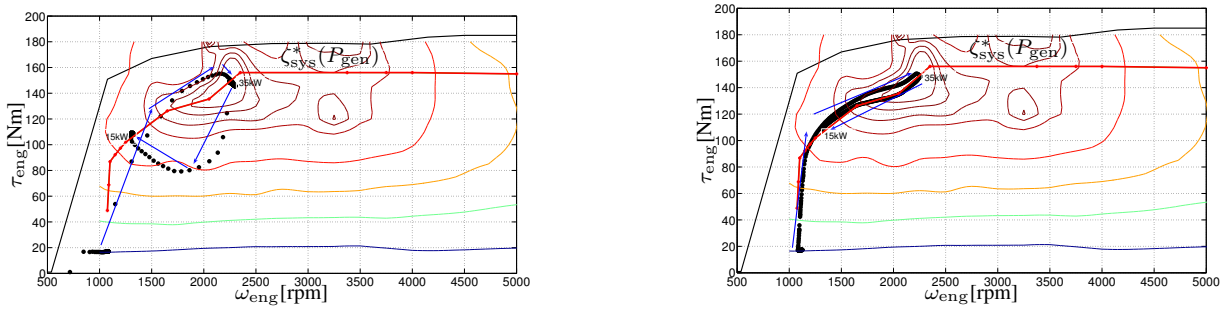

(a) Power steps from 2kW to 35kW, then to 15kW

(b) Power ramps from 2kW to 35kW then to 15kW

Fig. 2. Effect of abrupt and smooth transients on the engine operating point dynamics (optimal efficiency curve $\zeta^*_{\rm sys}$ in red).

i.e., at non-optimal efficiency. The simulation where the engine power ramps from 2kW to 35kW at 2.5kW/s rate and then to 15 kW at -1kW/s rate executed on the same environment is shown in Figure 2(b). In this case the engine operating point "slides" along $\zeta^*_{\rm sys}$.

Indeed, by performing a smoother transient -a ramp instead of a step- the lower-level control algorithm can maintain the engine close to the optimum efficiency curve. At every control cycle the energy management strategy commands a generator power transition $P_{\rm gen}(k) \rightarrow P_{\rm gen}(k+1)$ which is converted into an operating point transition $\zeta^*_{\rm sys}(P_{\rm gen}(k)) \rightarrow \zeta^*_{\rm sys}(P_{\rm gen}(k+1))$, consistent with

$$(\omega^*_{\rm eng}(k), \tau^*_{\rm eng}(k)) \rightarrow (\omega^*_{\rm eng}(k+1), \tau^*_{\rm eng}(k+1))$$

Due to continuity, if $\Delta P^*_{\rm gen}(k) = P^*_{\rm gen}(k+1) - P^*_{\rm gen}(k)$ is small, then $\Delta\omega^*_{\rm eng}(k) = (\omega^*_{\rm eng}(k+1) - \omega^*_{\rm eng}(k))$ and $\Delta\tau^*_{\rm eng}(k) = (\tau^*_{\rm eng}(k+1) - \tau^*_{\rm eng}(k))$ are small, and as a consequence the transients are reduced.

The power transients are responses to driver power requests changes which can be arbitrarily aggressive. However, the engine is not the only power source in the SHEV, and by (2) it is possible to smoothen its power transients by using the battery. In fact, since the electrical dynamics are faster than the mechanical ones, it makes sense to absorb rapid power variations by the battery, and to use the (slower) mechanical components to deal with the low frequency content of the power request.

On the other hand, the power that the battery can provide is limited, and the battery state of charge should be maintained within a desirable operating interval. Thus, the power-smoothing energy management strategy must be implemented in an algorithm that is capable of enforcing constraints on the actuator limits and on the components desired operating ranges, and of trading-off between different objectives, such as using the battery to smoothen the current transient, yet maintaining enough charge to absorb transients in the immediate future.

IV. MPC-based Power Smoothing Control

Model predictive control (MPC) is a successful strategy for controlling systems subject to input and state constraints, where the optimal trade-off between competing control objectives is sought. Hence, it appears to be a natural candidate for the power smoothing energy management strategy for the SHEV, where constraints on powerflow and battery charge have to be enforced, and where the trade-off between power smoothing and battery usage has to be optimized. Due to the capabilities of automotive ECUs, a linear MPC algorithm is used with a relatively short prediction horizon. In fact, nonlinear MPC is in general too complex for real-time implementation in automotive ECUs, while a short horizon is required because some of the relevant variables, e.g., wheel power request, cannot be reliably predicted for long in the future.

We design a discrete-time MPC controller with sampling period T_s that selects the generator power variation $\Delta P_{\rm gen}(k) = P_{\rm gen}(k+1) - P_{\rm gen}(k)$, where we also impose $\Delta P^{\rm min}_{\rm gen} \leq \Delta P_{\rm gen}(k) \leq \Delta P^{\rm max}_{\rm gen}$. In order to account for extreme accelerations and decelerations, we provide two additional control signals, $P_{\rm brk}$ and $P_{\rm xt}$, where $P_{\rm brk}$ is the power dissipated by conventional (friction) brakes, for the cases where regenerative braking is insufficient, and $P_{\rm xt}$ is an additional generator power request to be used in case of aggressive accelerations. As a consequence, the generator power dynamics are defined by

$$P_{\rm gen}(k+1) = P_{\rm gen}(k) + \Delta P_{\rm gen}(k) + P_{\rm xt}(k). \qquad (9)$$

The desired wheel power, which is computed basing on the current driver's pedal input and vehicle state, is converted into a desired bus power by (1), (2),

$$P_{\rm bus}(k) = \frac{P_{\rm wh}(k)}{\eta_{\rm mot}(k)\eta_{\rm wh}(k)}, \qquad (10)$$

that in the MPC controller is seen as a measured disturbance, assumed constant along the (brief) prediction horizon. Thus, by (2), (9), (10) the battery power can be expressed as

$$\begin{aligned} P_{\rm bat}(k) \;\; = \;\; & P_{\rm bus}(k) - P_{\rm gen}(k) - \Delta P_{\rm gen}(k) \\ & + P_{\rm brk}(k) - P_{\rm xt}(k). \end{aligned} \qquad (11)$$

The most relevant dynamics in the energy management [2] is the battery state of charge (SoC), which is defined as the percentage ratio between the (current) battery charge and

the maximum charge $SoC = 100 \cdot \frac{Q_{\rm bat}}{Q_{\rm bat}^{\max}}$. In this paper we slightly modify this definition into $SoC = 100 \cdot \frac{Q_{\rm bat} - Q_{\rm bat}^{\rm ref}}{Q_{\rm bat}^{\max}}$, hence shifting the zero of the state of charge at the desired SoC value $Q_{\rm bat}^{\rm ref}$. In order to implement an MPC algorithm that can execute in real time, we identify a linear autoregressive (ARX) model for the battery dynamics by using data from simulations of the high fidelity SHEV model. The identification procedure indicates that the integral model

$$SoC(k+1) = SoC(k) - \gamma P_{\rm bat}(k) \tag{12}$$

is satisfactory since it achieves a fit of more than 85% on the UDDS (Urban Dynamometer Driving Schedule) cycle. By increasing the model order (ARX up to 10 poles, 10 zeros), the identified models show pole-zeros cancellations, and less than 2% improvement. Thus, we use (12) counting on the capability of MPC to counteract model imperfections.

From (9), (11), (12), the MPC prediction model is

$$\begin{aligned} x(k+1) &= Ax(k) + Bu(k) && \text{(13a)} \\ y(k) &= Cx(k) + Du(k), && \text{(13b)} \end{aligned}$$

where $x = \left[\begin{smallmatrix} P_{\rm gen} & SoC & P_{\rm bus} \end{smallmatrix}\right]'$, $u = \left[\begin{smallmatrix} \Delta P & P_{\rm xt} & P_{\rm brk} \end{smallmatrix}\right]'$, $y = P_{\rm bat}$, and

$$A = \begin{bmatrix} 1 & 0 & 0 \\ \gamma & 1 & -\gamma \\ 0 & 0 & 1 \end{bmatrix}, \; B = \begin{bmatrix} 1 & 1 & 0 \\ \gamma & \gamma & -\gamma \\ 0 & 0 & 0 \end{bmatrix}, \; \begin{matrix} C = \left[\begin{smallmatrix} -1 & 0 & 1 \end{smallmatrix}\right], \\ D = \left[\begin{smallmatrix} -1 & -1 & 1 \end{smallmatrix}\right]. \end{matrix}$$

Basing on (13), the MPC optimal control problem is

$$\begin{aligned} \min_{U(k)} \quad & x(N|k)Px(N|k) + \sum_{i=0}^{N-1} x(i|k)'Qx(i|k) \\ & + u(i|k)'Ru(i|k) + y(i|k)'Sy(i|k) && \text{(14a)} \\ \text{s.t.} \quad & x(i+1|k) = Ax(i|k) + Bu(i|k) && \text{(14b)} \\ & y(i|k) = Cx(i|k) + Du(i|k) && \text{(14c)} \\ & \underline{x} \le x(i|k) \le \overline{x}, \; N = 0, \ldots, N_c && \text{(14d)} \\ & \underline{u} \le u(i|k) \le \overline{u}, \; N = 0, \ldots, N_u - 1 && \text{(14e)} \\ & \underline{y} \le y(i|k) \le \overline{y}, \; N = 0, \ldots, N_c && \text{(14f)} \\ & x(0|k) = x(k) && \text{(14g)} \\ & u(i|k) = Kx(j|k) \; i = N_u, \ldots, N-1 && \text{(14h)} \end{aligned}$$

where $U(k) = (u(0|k), \ldots, u(N_u - 1))$, N is the prediction horizon, $N_u \le N$ is the control horizon, and N_c is the constraint horizon. The state, input, and output bounds in (14d)–(14f) are

$$\overline{x} = \begin{bmatrix} P_{\rm gen}^{\max} \\ SoC^{\max} \\ \infty \end{bmatrix}, \; \underline{x} = \begin{bmatrix} P_{\rm gen}^{\min} \\ SoC^{\min} \\ -\infty \end{bmatrix}, \; \begin{matrix} \overline{y} = \left[\begin{smallmatrix} P_{\rm bat}^{\max} \end{smallmatrix}\right], \\ \underline{y} = \left[\begin{smallmatrix} P_{\rm bat}^{\min} \end{smallmatrix}\right], \end{matrix}$$
$$\overline{u} = \begin{bmatrix} \Delta P_{\rm gen}^{\max} \\ \infty \\ \infty \end{bmatrix}, \; \underline{u} = \begin{bmatrix} \Delta P_{\rm gen}^{\min} \\ 0 \\ 0 \end{bmatrix},$$

and the positive semidefinite cost matrix weights are

$$Q = \begin{bmatrix} 0 & 0 & 0 \\ 0 & q_{SoC} & 0 \\ 0 & 0 & 0 \end{bmatrix}, \; R = \begin{bmatrix} r_\Delta & 0 & 0 \\ 0 & \rho & 0 \\ 0 & 0 & \rho \end{bmatrix}, \; S = \left[\begin{smallmatrix} s_{\rm bat} \end{smallmatrix}\right].$$

Since $P_{\rm brk}$ and $P_{\rm xt}$ should be non-zero only on aggressive maneuvers, ρ is significantly larger than the other weights. The terminal state weight P in (14a) and the terminal gain K in (14h) can be set to zero, or used to improve stability properties, as explained later.

At every control cycle k, the MPC algorithm solves optimization problem (14) initialized by (14g) at the current measured/estimated state $x(k)$. The first element of the optimal control sequence $U^*(k)$, is used to compute the control input, the requested generator power, battery power and friction brake power, that are passed to the lower level controllers according to the implemented architecture,

$$v(k) = \begin{bmatrix} P_{\rm gen}(k) + [u^*(0|k)]_1 + [u^*(0|k)]_2 \\ P_{\rm bus}(k) - P_{\rm gen}(k) - [u^*(0|k)]_1 - [u^*(0|k)]_2 + [u^*(0|k)]_3 \\ [u^*(0|k)]_3 \end{bmatrix},$$

where $[u]_i$ is the $i-th$ component of vector u.

A. Terminal cost and engine efficiency approximation

In order to obtain local Lyapunov stability, the terminal cost in (14) can be used. To achieve this, the terminal weight P and terminal gain K can be selected basing on the LQR problem for the reduced order system

$$\begin{aligned} \tilde{x}(k+1) &= \tilde{A}\tilde{x}(k) + \tilde{B}\tilde{u}(k) && \text{(15a)} \\ & \tilde{A} = \left[\begin{smallmatrix} 1 & 0 \\ \gamma & 1 \end{smallmatrix}\right], \; \tilde{B} = \left[\begin{smallmatrix} 1 \\ \gamma \end{smallmatrix}\right] && \text{(15b)} \end{aligned}$$

where $\tilde{x} = \left[\begin{smallmatrix} P_{\rm gen} - P_{\rm bus} & SoC \end{smallmatrix}\right]'$, $\tilde{u} = \left[\begin{smallmatrix} \Delta P_{\rm gen} \end{smallmatrix}\right]$, and we use as LQR weights $\tilde{Q} = \left[\begin{smallmatrix} 0 & 0 \\ 0 & q_{SoC} \end{smallmatrix}\right]$, $\tilde{R} = \left[\begin{smallmatrix} r_\Delta \end{smallmatrix}\right]$ to match the cost in (14a) for subsystem (15). By solving the Riccati equation for (15) using $\tilde{Q}$, $\tilde{R}$, and obtaining $\tilde{P}$, $\tilde{K}$ as cost-to-go and LQR gain, one can construct the terminal cost and the terminal controller gain for (14) as $P = \tilde{C}'\tilde{P}\tilde{C}$, $K = \left[\begin{smallmatrix} (\tilde{K}\tilde{C})' & 0 & 0 \end{smallmatrix}\right]'$, where $\tilde{C} = \left[\begin{smallmatrix} 1 & 0 & -1 \\ 0 & 1 & 0 \end{smallmatrix}\right]$. For this choice of weights, whenever the constraints in (14) are not active and the power request is constant, say $P_{\rm bus}^e$, the MPC command is coincident with the LQR controller that stabilizes (13) on the equilibrium $x^e = [P_{\rm gen}^e \; SoC^e \; P_{\rm bus}^e]$, where $P_{\rm gen}^e = P_{\rm bus}^e$ and $SoC^e = 0$. The set where the constraints are inactive can be computed as indicated in [10].

If Lyapunov stability is not the primary concern, one can set $K = 0$ and $P = 0$ in (14) and modify (14a) to include an approximation of ${\eta_{\rm sys}^*}^{-1}$, that is, an approximation of the inverse engine-generator efficiency along the optimal curve $\zeta_{\rm sys}^*$. This is possible thanks to the power smoothing control algorithm that forces the engine to operate along $\zeta_{\rm sys}^*$. In cases such as the one shown in Figure 2(a) a one-dimensional approximation of the inverse efficiency is not appropriate because the engine-generator does not operate along a curve. In order to maintain (14) as a quadratic programming problem, a quadratic approximation of ${\eta_{\rm sys}^*}^{-1}$ is included in (14),

$$\tilde{\eta}_{\rm sys}(P_{\rm gen}(i|k)) = a_1 P_{\rm gen}(i|k)^2 + a_1 P_{\rm gen}(i|k) + a_0. \tag{16}$$

When (16) is included in (14a), the MPC controller trade-offs between the base smoothing power control objectives, and running at operating at the power where (16) is minimum, the maximum engine efficiency point. By adding a weight (i.e., by scaling the coefficients a_i, $i = 0, 1, 2$) the different performance trade-offs are found. However, (16) introduces a "bias" in the generator power and hence the closed-loop system does not necessarily stabilizes on x^e anymore, but it may results in a steady-state SoC offset.

B. Synthesis of the explicit MPC law

Although the MPC optimal control problem (14) results in a constrained quadratic program that can be easily solved at high rates in standard computers, real-time solution of (14) in standard automotive hardware may present computational problems. An important advantage of linear MPC is that the quadratic program (14) can be solved *explicitly* [9]. In this case the command is obtained by evaluating the control law

$$u = \gamma_{\mathrm{MPC}}(x) = \quad F_j x + G_j \tag{17a}$$

$$j: \quad H_j x \leq K_j \tag{17b}$$

where $j \in \{1, \ldots, s\}$, and matrices F_j, H_j and vectors G_j, K_j, for $j = \{1, \ldots, s\}$, are computed for instance by the algorithm in [9]. Control law (17) defines a continuous piecewise affine state feedback law, where (17b) defines a partition of the state space in s polyhedral regions, and (17a) defines the input function for each region. The computation of the input from (17) requires checking inequalities (17b) until $\bar{j} \in \{1, \ldots, s\}$ is found, such that (17b) is satisfied for $j = \bar{j}$, then the evaluation of (17a) for $j = \bar{j}$.

The explicit feedback law is also used to analyze the closed-loop system, obtained by substituting (17) in (13),

$$x(k+1) = (A + BF_j)x(k) + BG_j \tag{18a}$$

$$y(k) = (C + DF_j)x(k) + DG_j \tag{18b}$$

$$j: \quad H_j x(k) \leq K_j \tag{18c}$$

which is a piecewise affine dynamical system. The stability of (18) can be analyzed globally by using piecewise quadratic Lyapunov functions [11], and locally [12] by finding the region $\bar{\imath} \in \{1, \ldots, s\}$ that contains the origin, and computing the eigenvalues of $(A + BF_{\bar{\imath}})$. In this case, the domain of attraction is a set $\mathcal{X} \supset \mathcal{X}_{\mathrm{PI}}$, where $\mathcal{X}_{\mathrm{PI}}$ is the maximum positively invariant set contained in $SS_{\mathrm{PI}} = \{x : H_{\bar{\imath}} x \leq K_{\bar{\imath}}\}$ for dynamics $x(k+1) = (A + BF_{\bar{\imath}})x(k) + BG_{\bar{\imath}}$.

V. Implementation and Experimental Results

The controller designed in Section IV is first tested in simulation in closed-loop with a high-fidelity proprietary model that simulates not only all the vehicle subsystems - engine, vehicle dynamics, loads, etc.-, but also the whole control software that operates within the different ECUs.

We design the MPC controller with $T_s = 1$, where the terminal cost weight P and the terminal controller K in (14a) are set to zero, and the quadratic approximation of the efficiency (16) is used, resulting in the cost function

$$J = \sum_{k=0}^{N-1} r_\Delta \Delta P_{\mathrm{gen}}(i|k)^2 + \rho(P_{\mathrm{brk}}(i|k)^2 + P_{\mathrm{xt}}(i|k)^2) + s_{\mathrm{bat}} P_{\mathrm{bat}}(i|k)^2 + q_{SoC} SoC(i|k)^2 + q_\eta \tilde{\eta}_{\mathrm{sys}}(P_{eng}(k|t)).$$

where r_Δ, ρ, s_{bat}, q_{SoC}, q_η are positive weights. The constraint bounds are $P_{\mathrm{bat}}^{\min} = -30$kW, $P_{\mathrm{bat}}^{\max} = 40$kW, $P_{\mathrm{gen}}^{\max} = 80$kW, $\Delta P_{\mathrm{gen}}^{\max} = -\Delta P_{\mathrm{gen}}^{\min} = 11$kW, $SoC^{\min} = 40 - SoC_r$, $SoC^{\max} = 60 - SoC_r$, and $SoC_r = 50$ (note that SoC is in percentage). The constraints on the state-of-charge are "softened" to avoid infeasibility caused by unmodelled loads and uncertainties.

The simulations are used to select the main calibration parameters of the MPC controller, such as the length of the horizon and the weights in (14a). Basing on simulation results we choose horizons $N = 20$, $N_u = 4$, $N_c = 6$. Also, simulation results are used to select the range where electric-vehicle (EV) operation mode is enforced. We define a generator power threshold $P_{\mathrm{gen}}^{\mathrm{EV}}$ such that if $[u(k)]_1 \leq P_{\mathrm{gen}}^{\mathrm{EV}}$, the engine is turned off. $P_{\mathrm{gen}}^{\mathrm{EV}}$ is selected by analyzing the engine efficiency achieved in simulation, looking for the low power region where the efficiency drops sharply.

After verifying in simulations that the controller is implemented correctly, we have deployed it in the standard ECU, for experimental testing. In order to do this, we have synthesized the explicit MPC law (17), that in our application is composed of $s = 127$ regions, for a total of 589 inequalities. The controller uses about 2% of the available memory and less than 1% of the available computational capabilities, in the worst case. By analyzing the closed-loop system (18), we verified that the controller is locally stable under a constant bus power request, even though due to the use of (16), $SoC = 0$ is not guaranteed at the equilibrium.

The controller is experimentally tested on a fully functional and drivable series hybrid electric vehicle prototype in a dynamometer chassis roll, where a human driver follows the UDDS cycle reference. The focus of the test is the correct operation of the controller designed in Section IV and the evaluation of the impact on fuel consumption. To this end, the results of the controller are compared with two rule-based strategies, a load following one and a load-levelling one, calibrated by the results of dynamic programming [2] and ECMS [4]. Additional details on the base strategies and on the prototype vehicle are available on [13].

In Figure 3 we show the generator, battery, and motor power during two specific intervals of the UDDS cycle, where the power smoothing effects are evident. Initially, the engine is turned off. Then, when the engine is turned on at $t = 859$s, most of the bus power variations are absorbed primarily by the battery, while the generator power (and the engine power as a consequence) varies slowly, so that the engine operating point is maintained close to the optimal curve.

Figure 4(a) reports the velocity and the reference profile during the full cycle, showing that the velocity profile of the driving cycle is correctly tracked, and that the controller provides the requested power. Figure 4(b) shows the SoC time history during the full driving cycle. During a short interval around $t = 100$s, the minimum SoC constraint is violated by a small amount. This may happen due to unmodelled dynamics and uncertainties. However, since the SoC constraints are softened, the controller continues operating and recover rapidly, bringing the SoC back to the desired range. Figure 5 shows the engine operating point with respect to the optimal system efficiency curve η_{sys}^*. The operating points are all concentrated in a small band around η_{sys}^*,

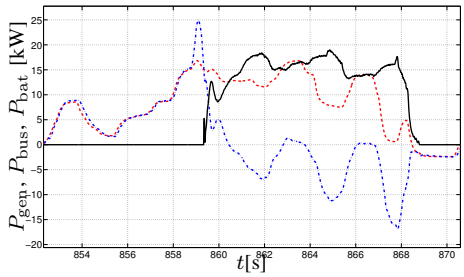

Fig. 3. Power transients $t \in [855, 871]$s during the UDDS cycle: generator power (solid), battery power (dash-dot), bus power (dash).

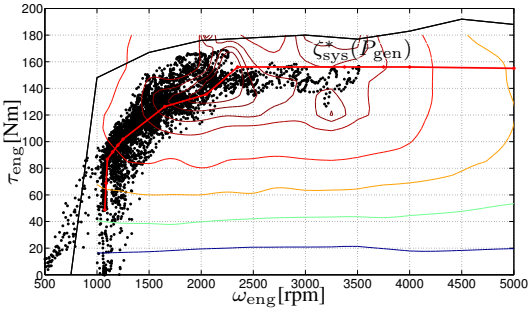

Fig. 5. Experimental results on UDDS cycle. Engine operating points, optimal efficiency curve $\zeta^*_{\rm sys}$, and iso-efficiency curves.

which is possible thanks to the transient smoothing behavior induced by the proposed controller. We have compared the fuel economy results over three executions of the cycle per each controller, and we have applied an empirical formula to adjust for the (small) difference between initial and final SoC. The proposed control strategy provides a fuel economy improvement of more than 4.5% with respect to the two base strategies.

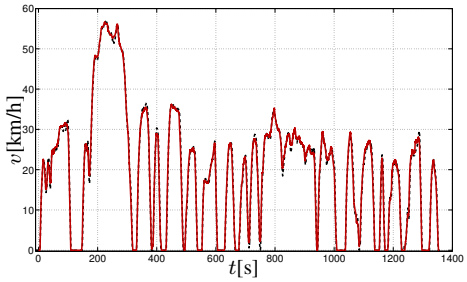

(a) Vehicle velocity (solid) and reference velocity (dashed).

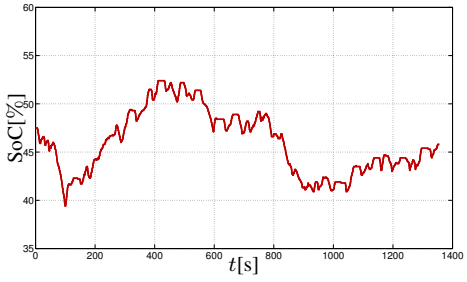

(b) Battery state of charge.

Fig. 4. Experimental results on UDDS cycle. Velocity and SoC.

VI. Conclusions

We have presented an energy management strategy that focuses on optimizing the engine efficiency for a series hybrid electric vehicle. While the stationary optimal efficiency is optimized by exploiting the fact that in the SHEV the engine is mechanically disconnected from the traction wheels, and hence its operating point can be arbitrarily chosen, the transients and their negative effects on fuel economy are reduced by using the battery as a buffer to smoothen the engine operating point variations. For this purpose, we have designed a model predictive controller that optimally manages the transients from one operating point to another. The experimental results executed on a fully functional vehicle on a chassis-roll dynamometer using the UDDS cycle show fuel economy improvements with respect to two base strategies.

References

[1] A. Sciarretta and L. Guzzella, "Control of hybrid electric vehicles," *IEEE Control Systems Magazine*, pp. 60–67, April 2007.

[2] L. Guzzella and A. Sciarretta, *Vehicle Propulsion Systems Introduction to Modeling and Optimization*. Springer Verlag, 2005.

[3] C. Lin, H. Peng, and J. Grizzle, "A stochastic control strategy for hybrid electric vehicles," in *American Control Conference*, vol. 5, no. 30, 2004, pp. 4710–4715.

[4] C. Musardo, G. Rizzoni, and B. Staccia, "A-ECMS: An adaptive algorithm for hybrid electric vehicle energy management," in *Proc. 44th IEEE Conf. on Decision and Control*, Seville, Spain, 2005, pp. 1816–1823.

[5] G. Ripaccioli, A. Bemporad, F. Assadian, C. Dextreit, S. Di Cairano, and I. Kolmanovsky, "Hybrid Modeling, Identification, and Predictive Control: An Application to Hybrid Electric Vehicle Energy Management," *Hybrid Systems: Computation and Control*, pp. 321–335, 2009.

[6] H. Borhan, C. Zhang, A. Vahidi, A. Phillips, M. Kuang, and S. Di Cairano, "Nonlinear model predictive control for power-split hybrid electric vehicles," in *Proc. 49th IEEE Conf. on Decision and Control*, Atlanta, GA.

[7] G. Ripaccioli, D. Bernardini, S. Di Cairano, A. Bemporad, and I. Kolmanovsky, "A stochastic model predictive control approach for series hybrid electric vehicle power management," in *American Control Conference*, Baltimore, MD, 2010, pp. 5844–5849.

[8] J. Maciejowski, *Predictive control with constraints*. Englewood Cliffs, NJ: Prentice Hall., 2002.

[9] A. Bemporad, M. Morari, V. Dua, and E. Pistikopoulos, "The explicit linear quadratic regulator for constrained systems," *Automatica*, vol. 38, no. 1, pp. 3–20, 2002.

[10] S. Di Cairano and A. Bemporad, "Model predictive control tuning by controller matching," *IEEE Trans. Automatic Control*, vol. 55, no. 1, pp. 185 –190, jan. 2010.

[11] G. Ferrari-Trecate, F. Cuzzola, D. Mignone, and M. Morari, "Analysis of discrete-time piecewise affine and hybrid systems," *Automatica*, vol. 38, pp. 2139–2146, 2002.

[12] S. Di Cairano, D. Yanakiev, A. Bemporad, I. Kolmanovsky, and D. Hrovat, "An MPC design flow for automotive control and applications to idle speed regulation," in *Proc. 47th IEEE Conf. on Decision and Control*, Cancun, Mexico, 2008, pp. 5686–5691.

[13] Q. Wang, W. Liang, M. L. Kuang, and R. McGee, "Vehicle system controls for a series hybrid powertrain," in *SAE World Congress*, Detroit, MI, 2011, to appear.